Available online at www.sciencedirect.com
ScienceDirect
International Journal of Heat and Fluid Flow 28 (2007) 191–202
International Journal of HEAT AND FLUID FLOW
www.elsevier.com/locate/ijhff

An experimental methodology to quantify the spray cooling event at intermittent spray impact ☆

António L.N. Moreira *, João Carvalho, Miguel R.O. Panão

Instituto Superior Técnico, Mechanical Engineering Department, Center for Innovation, Technology and Policy Research, IN+ Av. Rovisco Pais 1049-001, Lisboa Codex, Portugal

Received 21 August 2005; received in revised form 7 February 2006; accepted 22 March 2006
Available online 22 May 2006

Abstract

The present paper describes an experimental methodology devised to study spray cooling with multiple-intermittent sprays as those found in fuel injection systems of spark-ignition and diesel engines, or in dermatologic surgery applications. The spray characteristics and the surface thermal behaviour are measured by combining a two-component phase-Doppler anemometer with fast response surface thermocouples. The hardware allows simultaneous acquisition of Doppler and thermocouple signals which are processed in Matlab to estimate the time-varying heat flux and fluid-dynamic characteristics of the spray during impact. The time resolution of the acquisition system is limited by the data rate of validation of the phase-Doppler anemometer, but it has been shown to be accurate for the characterization of spray-cooling processes with short spurt durations for which the transient period of spray injection plays an important role. The measurements are processed in terms of the instantaneous heat fluxes, from which phase-average values of the boiling curves are obtained. Two of the characteristic parameters used in the thermal analysis of stationary spray cooling events, the critical heat flux (CHF) and Leidenfrost phenomenon, are then inferred in terms of operating conditions of the multiple-intermittent injections, such as the frequency, duration and pressure of injection.

An integral method is suggested to describe the overall process of heat transfer, which accounts for the fluid-dynamic heterogeneities induced by multiple and successive droplet interactions within the area of spray impact. The method considers *overall boiling curves* dependant on the injection conditions and provides an empirical tool to characterize the heat transfer processes on the impact of multiple-intermittent sprays. The methodology is tested in a preliminary study of the effect of injection conditions on the heat removed by a fuel spray striking the back surface of the intake valve as in spark-ignition internal combustion engines with port-fuel injection. Although the temperature at which the CHF occurs varies within the target surface, analysis shows that it remains constant when the heat flux is considered as a quantity integrated over the impacted area. For very short pulse durations (5 ms), the cooling efficiency is found to increase for low frequencies of injection and at the critical heat flux condition.

Keywords: Phase-Doppler anemometer; Spray impingement; Surface heat flux; Port-fuel injection

1. Introduction

The capability of spray impingement to remove large amounts of energy at low temperatures through the latent heat of evaporation is used in a wide range of engineering systems. Technological applications include those geared for surface cooling, such as metal foundries, high power electronic devices, or the skin in dermatologic laser surgery; or to promote fuel vaporization and gaseous mixing in internal combustion engines, either reciprocating or premixed-prevaporizing gas turbines. A considerable amount of experimental and theoretical work has been performed to develop heat transfer correlations based on steady state flow bench setups with heated surfaces, which provided valuable insights to the heat exchange between the surface

☆ Paper submitted to the International Journal of Heat, and Fluid Flow revised in January 2006.

* Corresponding author. Tel.: +351 21 841 7875; fax: +351 21 849 6156.
E-mail address: moreira@dem.ist.utl.pt (A.L.N. Moreira).

0142-727X/$ - see front matter © 2006 Elsevier Inc. All rights reserved.
doi:10.1016/j.ijheatfluidflow.2006.03.004

Nomenclature

A_γ	cross section area of measurement volume (m^2)
A_{impact}	spray impact area (m^2)
C_p	liquid specific heat (J/kg K)
D	drop diameter (μm)
D_{43}	volume-weighted mean droplet diameter (μm)
Ec	Eckert number ($U^2/(C_p\Delta T_{sat})$)
h_c	convection coefficient (W/m^2 K)
Ja	Jakob number ($C_p\Delta T_{sat}/L_{fg}$)
k	liquid thermal conductivity (W/m K)
L_{fg}	latent heat of evaporation (J/kg)
$\dot{m}_f$	liquid mass flux rate (kg/s)
$N(t)$	sample size at instant t
Nu	Nusselt number (h_cD/k)
Pr	Prandtl number ($C_p\mu/k$)
$\dot{q}''$	instantaneous heat flux (W/m^2)
$\langle\overline{\dot{q}''}\rangle_{max}$	maximum total time-average heat flux (W/m^2)
$\overline{\dot{q}''}$	time-average heat flux (W/m^2)
$\langle\overline{\dot{q}''}\rangle$	total time-average heat flux (W/m^2)
r	radial coordinate of the spray parallel to the wall (mm)
Re	Reynolds number ($\rho UD/\mu$)
T	temperature (°C)
U	drop axial velocity (m/s)
V	drop radial velocity (m/s)
We	Weber number ($\rho UD^2/\sigma$)

Greek symbols

γ	droplet direction ($\tan^{-1}(V/U)$, °)
ρ	liquid density (kg/m^3)
μ	liquid dynamic viscosity (kg/m s)
ε	spray cooling efficiency
σ	surface tension (N/m)
τ	time instant (s)
Δp_{inj}	injection pressure (bar)
Δt_{inj}	pulse duration (ms)
ΔT_{sat}	$\pm(T_w - T_{sat})$ – degree of superheating (+) or subcooling (−) (°C)
η_v	correction factor to account multiple scattering droplet inside measurement volume
ε_w	maximum deviation between the prescribed initial temperature and the temperature at the start of injection

Subscripts

fuel	relatively to the cooling liquid
r	reference
sat	liquid saturation point
w	wall

and spray droplets, as in Jia and Qiu (2003). It has been shown that heat transfer rates much higher than can be attained using pool boiling are possible with sprays since the vapour removal from the surface is more efficient. This leads to think that the thermal interaction between the spray droplets and the vapour during pre-impact have a significant influence on the heat transfer in spray cooling, as reported by Yoshida et al. (2001). González and Black (1997) studied the interaction between spray and buoyant jet arising from the heated surface and pointed out a considerable reduction in droplet velocity due to the counter-flowing buoyant vapour jet, although they used a relatively low range of Reynolds values (~800). It is therefore expected that the capabilities of spray cooling for intensive and accurately control heat removal can be enhanced with an injection system able to produce multiple-intermittent sprays by proper matching the duration and frequency of injection. A systematic investigation to optimize such procedure requires simultaneous measurements of droplet characteristics and surface thermal behaviour on impacting multiple-intermittent sprays.

Moreover, spray impingement against hot surfaces occur in other practical situations, which also require a comprehensive knowledge of the energy flow pathways that determine the surface temperature and the interaction of the liquid spray with the surface. One example deals with the development of fuel injection systems in internal combustion engines, as reported in Panão and Moreira (2005b): (i) a spark ignition engine with port fuel injection, fuel injection often targets the back of the intake valve to promote fuel vaporization, since the intake valve is both the hottest part in the intake system and also it is the fastest to come up to a higher temperature in the engine-warm-up process; however, a significant portion of the fuel injected during engine-warm-up deposits onto the port surfaces and generates a thin film, which does not have sufficient time to vaporize prior to the intake stroke and thus leading to unburned hydrocarbons in the exhaust gas. (ii) In direct injection engines, fuel impingement onto the piston head may be intentionally used to control the spatial distribution of the spray within the cylinder, or is to be avoided to promote a homogeneous ignitable mixture, depending on the mode of operation. In all cases impingement of the fuel spray onto interposed surfaces affects mixture preparation and, therefore, the performance of the engine.

Most of previous experiments performed on IC engines focused on post-impact behaviours, such as the heat flux between the spray and the target surface, based on surface temperature measurements (Shayler et al., 1996; Cowart and Cheng, 1999). Only a few considered the interrelation between heat transfer and droplet characteristics of the impinging spray, which required the use of simplified laboratory configurations where some of the complexities of practical flows were removed, even though considering IC

fuel injection systems, as in Arcoumanis and Chang (1993) and Cutter (1996). However, simultaneous measurements of the flow and heat transfer effects have not been provided yet, which again are still required in order to account for the effects of the transient nature of fuel injection systems.

In this work, a post-process algorithm is devised to synchronize data acquired simultaneously by a temperature acquisition system and a phase-Doppler anemometer (PDA). The algorithm is implemented in Matlab and applied to an intermittent gasoline spray impacting perpendicular onto a heated surface and the results are processed to obtain the instantaneous heat fluxes, from which phase-average values of the boiling curves are obtained. The critical heat flux and Leidenfrost phenomenon associated with local maximum and local minimum in the boiling curves are usually used to describe the different heat transfer regimes "experienced" by individual droplets upon impact, as noted in Naber and Farrell (1993). However, although in a poly-dispersed spray, surface temperature may be quoted as the single most important parameter determining the different heat transfer regimes, other parameters associated with multiple drop impact interference, such as successive impacts of droplets on top of others, collision of droplet films during spreading and lamella interaction affecting the crown development in neighbouring splashing droplets, may have an important role in the impingement outcome, as well as in the wall heat transfer. In the case of multiple-intermittent sprays, an additional parameter is the unsteadiness associated with droplets characteristics before, along and after the end of the electronic pulse commanding the opening and closing of the injector.

The work reported here follows earlier studies performed on the transient behavior of the fluid–dynamic interaction between a pulsed spray and a flat surface at ambient temperature (Panão and Moreira, 2004, 2005a). The interrelation between the fluid–dynamic and thermal mechanisms was further studied based on simultaneous measurements of instantaneous droplet characteristics and surface temperature and heat transfer (Panão and Moreira, 2005b). The results showed that the heat transfer regimes strongly depend on the injection conditions, such as pressure, duration and frequency. Here, an empirical correlation for the instantaneous spray/wall heat transfer is derived, which relates the Nusselt with the Reynolds and the Jakob numbers for a wide range of experimental conditions. Moreover, an empirical integral methodology is devised to allow describe the heat transfer over the entire area of spray impact which accounts for the interaction between multiple neighboring droplets.

2. Instrumentation and data processing

2.1. Experimental arrangement

The experimental setup was built to study the impingement of a gasoline spray onto a flat plate under cross-flow conditions, though the results reported here consider the spray into quiescent environment. The injector is a BOSCH pintle-type with 0.79 mm of pintle diameter inserted in a hole with 0.9 mm. The fuel spray has a hollow-cone structure with interior and exterior angles of 8° and 19°, respectively, measured with a laser-sheet flow visualization technique. The frequency and duration of injection are controlled by an arbitrary function generator (NI5411 from National Instruments Corporation). The injector has electromechanical delays relatively to the electronic pulses sent to open and close the pintle, which were determined to be 1.6 and 1.3 ms, respectively, and found to be independent of pressure and injection duration. Therefore, the effective injection period is always 0.3 ms shorter than expected. The fluid injected is commercial gasoline with density of 758 kg/m^3, dynamic viscosity of 4.66×10^{-4} kg/m s, refractive index of 1.44, surface tension of 19.4 mN/m, saturation temperature (T_{sat}) is assumed to be 60 °C and the latent heat of evaporation to be 346 kJ/kg. The injector is located at the top of a rectangular test section as shown in Fig. 1 (Panão and Moreira, 2002).

The impinging aluminium plate is located 55 mm below the injector nozzle and is 12 mm thick to avoid that fluctuations from the spray cooling event perturb the temperature at the bottom surface, which is kept constant for heat flux measurement purposes. The plate has a thermal diffusivity of 6.676×10^{-5} m^2/s and a thermal conductivity of 164 W/m K (Bejan, 1993). The target is heated by an electric resistance isolated at the bottom.

The temperature of the surface is measured by three fast-response eroding-type thermocouples, manufactured by Nanmac Corporation (Massachussets, USA), displaced in an L-shape with a 20 mm spacing. The junctions of the thermocouples are made by rubbing the surface with an abrasive cloth until the thermocouple resistance is between 8 and 12Ω to insure a response time in the order of 10 μs. A thermographic analysis showed that the thermocouples do not alter the uniform temperature distribution of the

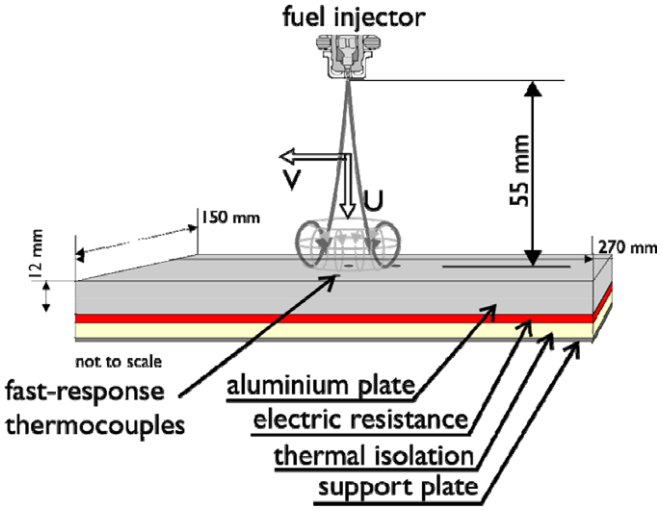

Fig. 1. Flow configuration (U, V – positive droplet axial, and radial, velocity, respectively).

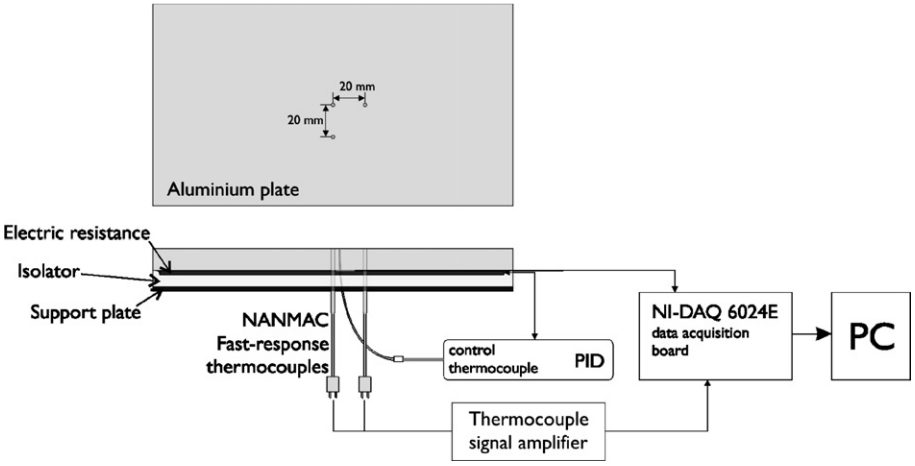

Fig. 2. Temperature data acquisition system.

Table 1
PDA optical configuration

Transmitting optics	Value
Laser power	300 mW
Wavelengths	514.5 and 488 nm
Beam spacing	60 mm
Transmitting focal length	500 mm
Frequency shift	40 MHz
Receiving optics	
Scattering angle	30°
Receiver focal length	500 mm
Processor parameters	
U and V signal bandwidth	12 MHz
S/N validation	0 dB
Spherical validation	10%

target. The thermocouple signals are amplified with a gain of 300 and digitized at a sample rate of 50 kHz. Electronic noise is quantified to be of the order of ±0.8 °C, significantly lower than the order of magnitude of the measured temperatures, as well as of the temperature decays caused by spray cooling. The system used to measure the wall temperature is schematically shown in Fig. 2.

Local time-resolved measurements of droplet size, velocity and flux are simultaneously measured with a two-component phase-Doppler DANTEC system consisting of a 55X transmitting optics, a 57×10 PDA receiving optics. The axial (U) and radial (V) velocity directions are represented in Fig. 1 and more details about the PDA optical configuration are described in Table 1. All the PDA measurements reported here were made at 5 mm above the target.

2.2. Experimental procedure

Electrical voltages from the thermocouples are read into computer memory through a plug-in data acquisition board (DAQ) with eight channels that contains analog-to-digital converters. Data acquisition is controlled by a program developed in Matlab. Doppler signals are acquired and processed for droplet diameter, two velocity components and fluxes by a 58N10 DANTEC Covariance processor. Each measurement system uses a separate computer, but both are triggered by the same electronic pulse used to trigger fuel injection. This signal is further used for timing purposes as the start of injection (SOI). An ideal sampling procedure could be devised, which samples continuously both signals up to achieve sampling sizes large enough for the resulting processed measurements to be statistically independent. However, this is not possible due to two orders of constraints.

The former is that validated Doppler signals are sampled at a much slower rate than temperature signals. An adequate sample size of Doppler signals would, therefore, exceed the maximum sample size in the DAQ computer board of temperature data. The second order of constraints derives from the fact that the heating system can not keep the surface temperature constant at the start of each injection. A practical sampling procedure must then consider these two issues: (1st) a reasonable sample size of validated Doppler signals and (2nd) a constant surface temperature at SOI. The first issue is accomplished by performing a series of n injections, being the number of series dependent on the required sample size. The second issue is accomplished by stating a maximum deviation between the prescribed initial temperature and the temperature read at SOI by the three surface thermocouples, ε_w.

$$\varepsilon_w = \left(\frac{T_w^{1st} - T_w^{ith}}{T_w^{1st}} \right) \times 100\% \quad (1)$$

The measurements reported here consider a maximum deviation of $\varepsilon_w = 1.5\%$. Therefore, the nth injection of each series is achieved when the target temperature at SOI is 1.5% below the temperature at the start of the 1st injection.

Fig. 3 shows the deviation of the target temperature at SOI along several series of 20 injections, for different injection conditions (duration and pressure of injection) when the initial target temperature is $T_w^{1st} = 150\,^{\circ}C$. The figure

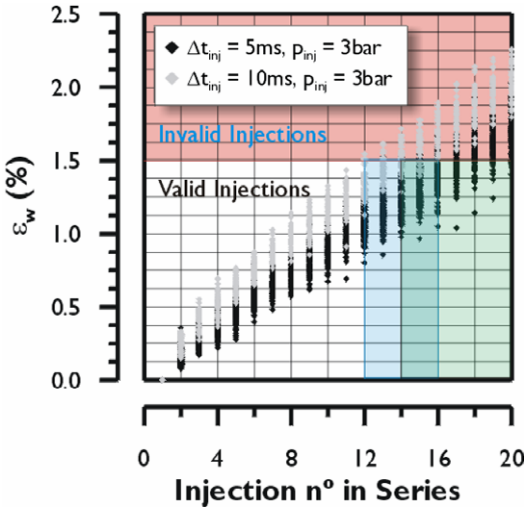

Fig. 3. Wall temperature decay along 20 injections for several injection conditions (duration and pressure of injection) when the initial target temperature is $T_w^{1st} = 150\ ^\circ C$.

shows that the number n of allowed injections should be around 12–16 for duration of injection of 10 ms and 14–20 for duration of injection of 5 ms.

Based on these criteria, the number n of injections in each series is prescribed at 20 injections and the number of series is chosen depending on the validation rate of Doppler signals.

2.3. Data acquisition and synchronization algorithm

Fig. 4 depicts the procedure of data acquisition: the transistor–transistor logic (TTL) signal generated by the function generator to trigger the fuel injector is used as a reset pulse for, both, the temperature and the Doppler acquisition systems. Once the acquisition program is started, the DAQ board continuously monitors the thermocouples signals waiting for a trigger from the function generator to start measuring.

After a series of injections, another program downloads the temperature data from the DAQ board, but instead of the complete dataset, it only downloads data acquired between an instant before the reset pulse (BRP) up to an instant right after the start of the injection (ASOI) pulse. These instants were set in our experiment to 5 (BRP) and 50 ms (ASOI), respectively. The 5 ms acquired before the pulse are used to calculate the wall temperature at the beginning of an injection cycle and also to check if the temperature distribution is uniform over the impact surface. While in the temperature acquisition system each injection is recorded in a different data file, for the PDA data a whole series is recorded. A procedure is then followed to generate a file of synchronized data from the individual data sampled, as shown in Fig. 5.

At a first step, the reset pulse of the first injection is used as a time frame to synchronize both data file. Then, at a second step, the n reset pulses of the n injections in each series are picked to be used as time frames to perform phase-average calculations. Finally, after applying a moving average to the temperature profile at step 3, two tasks are performed in order to reduce the effects of electronic noise: (task 1) calculate the wall heat flux from the temperature profile according to Reichelt et al. (2002); (task 2) at each instant a droplet is validated, the wall temperature and the wall heat flux are calculated by interpolation. The second task considers that the temperature is equivalent to a continuous phase in a multiphase flow, as exemplified in Fig. 6.

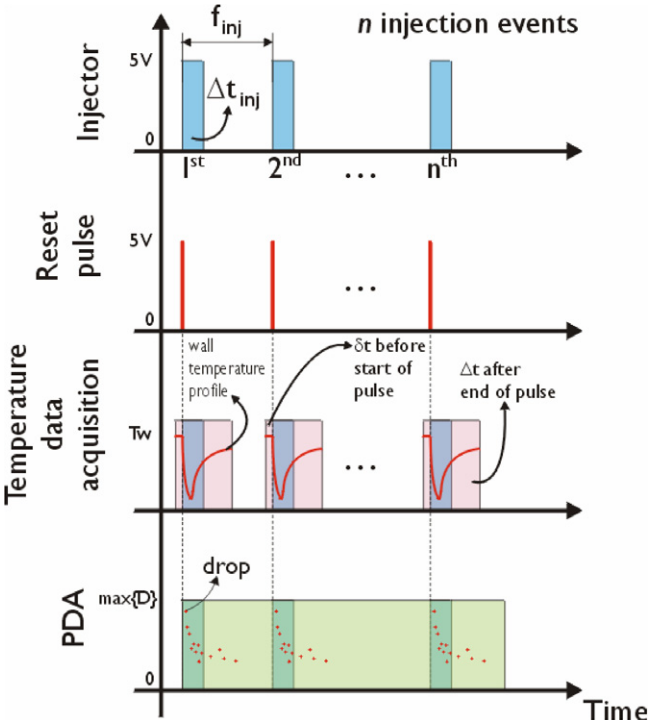

Fig. 4. Temporal diagrams for simultaneous measurements of wall temperature, size and velocity of droplets in each series of n injections.

The method to determine the heat flux profile assumes a uniform temperature distribution prior to spray impingement, a constant temperature at the bottom surface of the impinging plate and unidirectional conduction perpendicular to the surface.

The validity of assuming 1D heat conduction depends on negligible lateral heat conduction effects evaluated at the thermocouple junction and its outer boundaries. The eroding type fast response thermocouples are made of two ribbons of chromel and alumel, insulated by mica sheet, surrounded by the same material as the wall where it is embedded and, finally, packed in a 304SS alloy ultra-thin tube. Lateral heat conduction may occur at: δr for small perturbations near the thermocouple junction; and at thermocouple boundaries by the overall thermal resistance (R_t) due to the presence of different materials.

In the vicinity of the thermocouple junction, setting δr equal to 10% of the thermocouple radius and following the approach described in Buttsworth and Jones (1998),

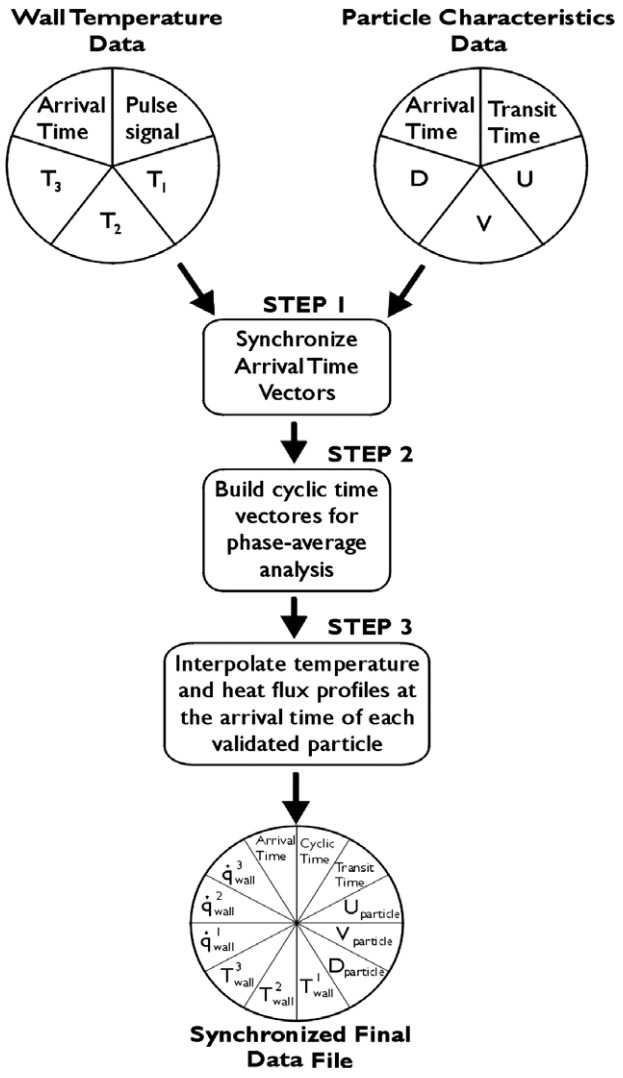

Fig. 5. Diagram of the procedure of generating a data file of synchronized data.

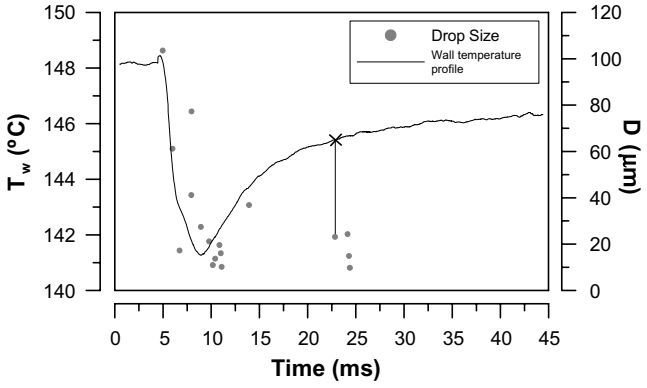

Fig. 6. Temporal evolution of the wall temperature and the associated temperature at the moment a droplet crosses the PDA detection volume for an injection.

the lateral heat conduction per unit area, $\dot{q}''^{\delta r}_{\mathrm{l}}$, is evaluated and compared with the instantaneous heat flux calculated by the Reichelt et al. method (2002), $\dot{q}''^{0}_{\mathrm{1D}}$. The residual sum of squares between $\dot{q}''^{0}_{\mathrm{1D}}$ and $\dot{q}''^{0}_{\mathrm{1D}} - \dot{q}''^{\delta r}_{\mathrm{l}}$ had median value of 0.223, which means that lateral heat conduction effects are negligible near the thermocouple junction. At the thermocouple boundaries ($r_{\mathrm{tc,bound}}$), the overall thermal resistance R_{t} is given by

$$R_{\mathrm{t}} = \frac{r_{\mathrm{tc}} - \delta r_{304\mathrm{SS}}}{k_{\mathrm{w}}} + \frac{\delta r_{304\mathrm{SS}}}{k_{304\mathrm{SS}}} \tag{2}$$

where r_{tc} is the radius of the thermocouple (1.5875 mm), $\delta r_{304\mathrm{SS}}$ is the thickness of the stainless steel pack (0.186 mm), k_{w} and $k_{304\mathrm{SS}}$ are the thermal conductivities of the aluminium and stainless steel alloy, 164 W/m K and 13.5 W/m K, respectively. And, estimating the surface temperature $T_{\mathrm{w}}^{r_{\mathrm{tc,bound}}}$ by linear interpolation of measurements from adjacent points, the lateral heat flux generated by R_{t} can be compared with $\dot{q}''^{0}_{\mathrm{1D}}$ as

$$\frac{T_{\mathrm{w}}^{\mathrm{junction}} - T_{\mathrm{w}}^{r_{\mathrm{tc,bound}}}}{R_t \cdot \dot{q}''^{0}_{\mathrm{1D}}} \times 100\% \tag{3}$$

and the resulting deviations were found to be ±0.08%, therefore, negligible.

Details about the deduction of the algorithm used to calculate the wall heat flux were reported by Reichelt et al. (2002) who also showed good agreement with the analytical solution for a semi-infinite body with a sinusoidal variation of temperature at the surface, for frequencies greater than 500 Hz. Our experiments are well above this limit and, therefore, inaccuracies are expected to be negligible. Moreover, the time resolution of the method can only be questioned in the low frequency regimes of the order of 0.1 Hz, as pointed out by Chen and Nguang (2003).

Once the three steps are completed, the final output data file contains the following information for each validated droplet: arrival time; cyclic time; transit time; axial and radial velocities; size; wall temperature measured by the three thermocouples ($T_{\mathrm{w}}^{1\text{ and }3}$ – lateral positions, T_{w}^{2} – central position, align with the injector central axis); and the wall heat flux removed by the spray at each thermocouple position ($q_{\mathrm{w}}^{1,2\text{ and }3}$). Examples of T_{w}^{2}, axial velocity and V–U correlation from a synchronized output file are shown in Fig. 7. It is noteworthy to observe that the axial velocity profile and the V–U correlation show a considerable number of droplets with a negative axial velocity generated by secondary atomization at the heated wall. Here, because the PDA measurement volume is located 5 mm above the target, the exact time and location of impact at the surface is obtained by extrapolation of the measured velocity vectors. This procedure does not affect the accuracy of the analysis, since the Stokesian response time of droplets (estimated as $\tau_{\mathrm{d}} = \rho D^2/[18\mu_{\mathrm{air}}]$) is much larger than the transit time between the PDA measurement volume and the surface for the impinging droplets.

2.4. Phase-average analysis

Phase average analysis is performed within time windows of 0.5 ms and with a minimum of 200 samples result-

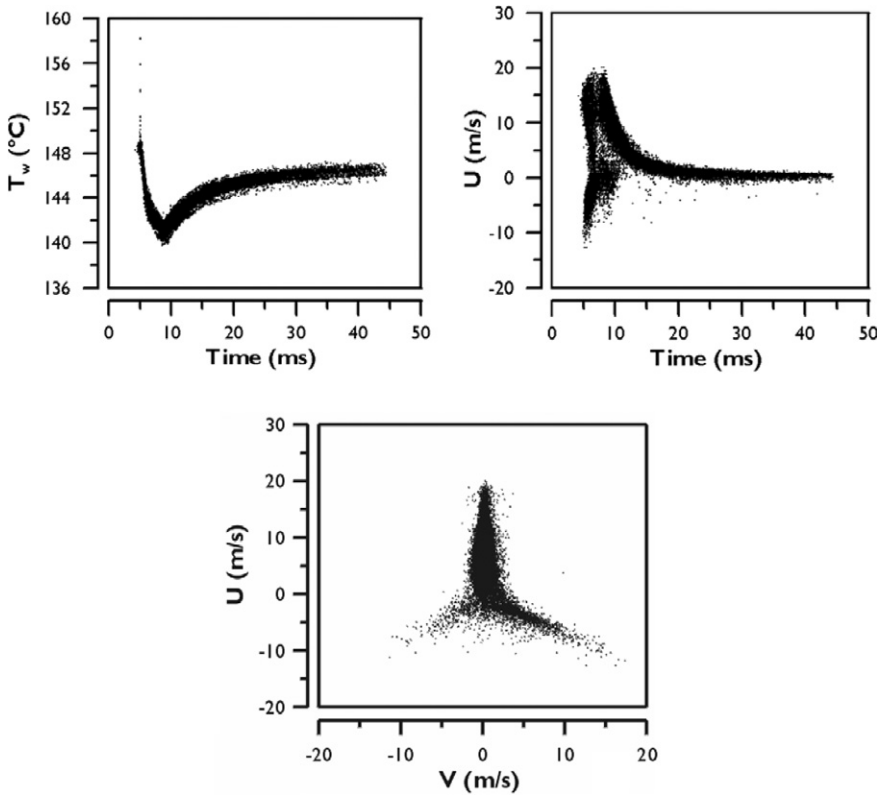

Fig. 7. Examples of temperature and axial velocity temporal profiles and a V–U plot for a synchronized output data file.

ing in an inaccuracy better than 9.4% in mean drop size (Tate, 1982) and better than 10% in PDA flux measurements (Saffman, 1987). Table 2 describes the quantities considered in the analysis.

In Table 2, β is an arbitrary quantity, which in the case of the PDA flux calculation may be the number, mass, momentum, kinetic energy or surface energy flux at time t. $N(t)$ is the sample size at time t, D_{ij} is the droplet mean diameter, η_{vi} is a correction factor considering multiple scattering due to the presence of more than one droplet inside the detection volume, $A_\gamma(D_k, \gamma_k)$ is the cross section area of the measurement volume, which is size and direction dependent (for more details on η_{vi} and $A_\gamma(D_k, \gamma_k)$, see Roisman and Tropea, 2001), and, finally, γ is the particle direction defined as $\gamma = a\tan(V/U)$. The post-process algorithm calculates other flow characteristics, but only those described in Table 2 where considered in the present analysis.

Table 2
Quantities used in phase-average analysis

Quantity	Expression
$T_w, \dot{q}''_w, \langle U \rangle$	Ensemble average: $\langle\beta\rangle(t) = \frac{1}{N(t)} \sum_{i=1}^{N(t)} \beta_i$
D_{43}	$D_{ij}(t) \frac{\sum_{i=1}^{N(t)} D^i}{\sum_{i=1}^{N(t)} D^j}$
PDA flux quantities	$\dot{B} = \frac{1}{\Delta t} \sum_{i=1}^{N_{sv}} \frac{\eta_{vi} \cdot \beta_i \cdot \cos(\gamma_i)}{A_\gamma(D_k, \gamma_k)}$

3. Results and discussion

The results are presented and discussed in this section under two headings. The first is aimed at deriving a correlation for the Nusselt number, which can be used to predict the thermal behavior of intake valves in port-fuel injection systems. The analysis is based on simultaneous measurements of droplets characteristics and surface thermal behavior measured at the axis of the spray, $r = 0$, and previously reported (Panão and Moreira, 2005b). The experimental conditions consider single injections to avoid interaction between successive injections and surface temperatures up to 150 °C, which are typical to those occurring in the back surface of the intake valve in the period of engine warm up (comparison on Table 3). In each temperature case, the pulse durations used were 5 and 10 ms and the injection pressures were 3 and 4.5 bar.

For transition and Leidenfrost heat transfer regimes, the new spray/wall heat transfer ceases to be valid, therefore, in the second sub-section, an integral method is devised to describe the overall process of heat transfer, which accounts for the heterogeneities of fluid–dynamic interactions induced by multiple and successive droplet interaction within the entire area of spray impact. Here, the

Table 3
Comparison between the surface temperature in the present experimental conditions and typical values found in the intake valve back-surface of SI engines during warm-up

Experimental conditions	Present work	Bauer et al. (1997)	Cowart and Cheng (1999)	Alkidas (2001)
Surface temperature (°C)	50, 150	<125	<100	<180

emphasis is put on the effects of engine operating conditions associated with the temperature of the impacted surface, the frequency of injection (engine speed), duration and pressure of injection, although the latter two were kept constant during experiments.

3.1. Spray/wall heat transfer correlation in gasoline-like conditions

The most relevant work on the development of spray/wall heat transfer correlations relevant for an engine-like environment was reported by Arcoumanis and Chang (1993, 1994) and Arcoumanis and Cutter (1995), but considers diesel conditions. However, diesel-oil has physical properties different from those of gasoline, and Diesel-injection is made at much higher pressures, which significantly alters the fluid-dynamics of the spray at impact (Mundo et al., 1995). In addition, the aforementioned research works based their analysis on independent measurements of droplet and surface thermal characteristics, namely droplet velocity and size were measured for the spray issuing into a quiescent atmosphere where the plate would be located. But an accurate analysis requires simultaneous measurements at the same location, even because it has been shown recently (Panão and Moreira, 2005a) that interposition of a surface alters the structure of the spray before impact. Therefore, more experimental evidence is needed to develop new or refine existing correlations, to accurately predict spray-valve heat transfer in spark-ignition engines, as also stressed by Lindgren and Denbratt (2000).

The heat transferred at the impact of a spray onto a surface depends on the thermo-physical properties of the liquid and on the temperature of the surface, as well as on size, velocity and mass flux of impinging droplets. The first two determine the heat transfer regime in accordance with the classical boiling theory, which includes film evaporation, nucleate/boiling, transition and film boiling, as qualitatively illustrated in Fig. 8. The size and velocity of droplets at impact determine the impingement outcome, i.e. if an impinging droplet sticks, rebounds, spreads, or splashes on the surface and, consequently, the contact time available for thermal interaction.

Therefore, the arbitrary relationship between the above mentioned parameters can be expressed as:

$$f(h_c, D, U, \rho, k, \mu, C_p, \sigma, L_{fg}, \Delta T_{sat}) = 0 \quad (4)$$

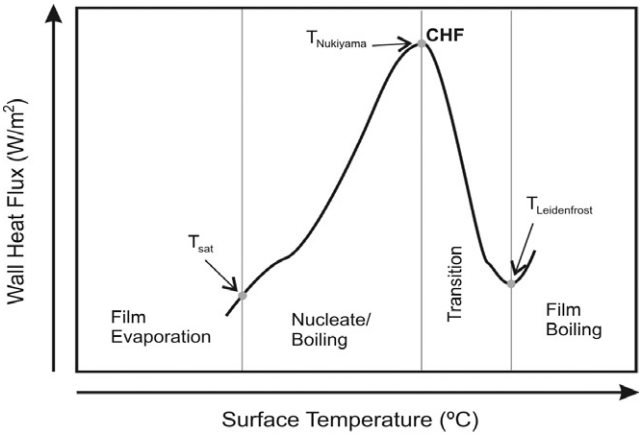

Fig. 8. Typical boiling curve and heat transfer regimes.

where h_c is the convection coefficient, D is the droplet diameter, U is the axial velocity and ΔT_{sat} is the difference between the wall temperature and the liquid saturation temperature at ambient pressure or sub-cooling temperature. The thermo-physical properties of the liquid are the specific mass (ρ), thermal conductivity (k), dynamic viscosity (μ), specific heat at constant pressure (C_p), surface tension (σ) and the latent heat of evaporation (L_{fg}), when the heat is removed from the surface by droplet vaporization.

Dimensional analysis allows deriving the variables of an empirical correlation for the instantaneous spray impingement heat transfer. It is noteworthy at this point that most heat transfer correlations developed for internal combustion engines concern the convective heat transfer and have been described in the following form:

$$Nu = aRe^m Pr^n \quad (5)$$

where Re ($=\rho UD/\mu$) is the Reynolds number and Pr ($=\mu \cdot C_p/k$) is the Prandtl number.

However, Arcoumanis and Chang (1993), purpose a new form for such a correlation, which includes a dimensionless group formed with the surface tension, to account for the stabilizing hydrodynamic force acting during droplet deformation, and for the effect of liquid spreading over the surface. This nondimensional group is expressed in the empirical correlation by the Weber number ($We = \rho U^2 D/\sigma$):

$$Nu = aRe^m Pr^n We^p \quad (6)$$

In the present work, two more parameters are suggested to be included: the latent heat of evaporation (L_{fg}) and the difference between the wall and liquid saturation temperatures (ΔT_{sat}), due to their importance in the definition of each heat transfer regime. Considering this, Eq. (4) reduces to six dimensionless groups: the Nusselt ($Nu = h_c D/k$), Reynolds, Prandtl and Weber numbers, as well as $c_p \cdot \Delta T_{sat}/L_{fg}$ and $U^2/c_p \cdot \Delta T_{sat}$:

$$f'\left(\frac{h_c D}{k}, \frac{\rho UD}{\mu}, \frac{C_p \cdot \mu}{k}, \frac{\rho U^2 D}{\sigma}, \frac{C_p \cdot \Delta T_{sat}}{L_{fg}}, \frac{U^2}{C_p \cdot \Delta T_{sat}}\right) = 0 \quad (7)$$

The last two groups are the Jakob (Ja) and the Eckert (Ec) numbers. The Jakob number represents the ratio of the sensible to the latent heat, the sensible heat being associated the degree of subcooling ($T_{sat} - T_w$), or superheat ($T_w - T_{sat}$), experienced by the liquid film formed after spray impact. The Eckert number is a measure of the relative importance of viscous-energy-dissipation during droplet deformation over the wall to the heat transfer analysis. The new proposed correlation is then expressed as:

$$Nu = aRe^{m}Pr^{n}We^{p}Ja^{q}Ec^{w} \tag{8}$$

Choi and Yao (1987) showed that in a dense spray, such as the present one, the Weber number of impinging droplets does not significantly affect the heat transfer. In addition, the Eckert has been observed to be of the order of 10^{-6} times smaller than Re for all the experiments reported here and, therefore, the viscous-energy dissipation can be neglected. Furthermore, the choice of appropriate velocity and size scales to calculate the dimensionless numbers is not obvious, though it is crucial to the accuracy of the correlation. In what concerns the first, the experimental evidence is that the drop axial velocity is the most appropriate characteristic velocity. Concerning the second, since the heat exchanged with the surface depends mainly on the mass flux of liquid (Yao and Choi, 1987), it is expected that the volume-weighted mean diameter, D_{43}, be appropriate as the characteristic size, as also suggested by Sowa (1992). After neglecting Ec and We numbers, the correlation that best fits the experimental results within the entire period of gasoline injection is given by:

$$Nu = 3.4 \times 10^{-5} \frac{Re^{1.51}}{Ja^{0.254}} \tag{9}$$

The proposed correlation has a coefficient of determination $R^2 = 0.89$, indicating that 89% of the dataset is predicted by the correlation and the uncertainty was estimated to be ±26%. The results given by Eq. (9) are compared in Fig. 9 with those obtained with the empirical correlation derived in Arcoumanis and Chang (1993). The discrepancies clearly show that the higher heat fluxes measured by Arcoumanis and Chang (1993) with a high-pressure Diesel spray cannot be described by the correlation derived here for a multi-point gasoline injection, where the impacting spray is characterized by larger droplet sizes with smaller velocities.

Furthermore, it was experimentally observed that the heat flux removed at the surface correlates with spray characteristics at impact only if the entire surface is at the nucleate boiling regime. This is attributed to the fact that the heat flux within that regime depends on the relative magnitude of the several forces acting upon each individual droplet at impact, since these determine the contact time available for thermal interaction and only weakly depend on the relative magnitude of momentum to thermal diffusivities. Since similarity occurs, the convective heat transfer can be outlined in terms of functional relations for the Nusselt number expressed in terms of dimensionless groups

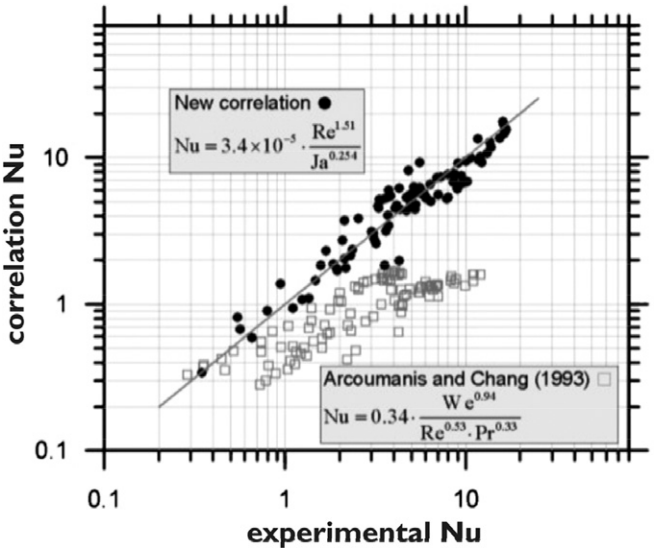

Fig. 9. Comparison between the empirical correlations for the Nusselt number.

scaling the several physical fluid and flow properties. The appropriate groups were found here to be the Reynolds and the Jacob numbers.

However, the heat transfer rate varies within the impacted area and therefore temperature gradients are generated during the cooling period. If the target is initially above the Nukiyama temperature, those gradients may be large and cause significant variations of the heat transfer regimes within the impact surface. The outcome of spray impact is then dominated by interactions between fluid-dynamic mechanisms at cold spots and pressure forces induced by bubble nucleation at neighbouring hot spots. The consequence is that similarity arguments do not apply and functional relations based on dimensionless groups cannot be found for the convective coefficient. A new methodology of analysis is then required if the vaporization rate is to be accurately predicted and that is the question addressed in the next paragraph.

3.2. Integral method of heat transfer analysis over the entire area of spray impact

It was shown in Panão and Moreira (2005b) that the temperature of Nukiyama at which the heat flux is maximum and the temperature of Leidenfrost at which it is minimum, vary within the area of impact due to non-uniformity of the flow regimes induced by interactions between neighboring and successive droplets. It was then suggested to devise an integral methodology by defining *overall boiling curves* similar to that in Fig. 8 to predict the average heat flux for several injection conditions (pressure, duration and frequency). This is the objective of the experiments reported in this subsection. Such a methodology would provide an empirical tool to optimize the heat transfer at the back surface of the intake valve in port-fuel injection systems so to avoid, as much as possible, the

formation of liquid films, which are one of the major sources of Hydrocarbons (HC) emitted into the atmosphere in the exhaust stroke.

Here, since the relevance of the analysis is for steady operating conditions after the engine warms up, the experiments were conducted for surface temperatures of 125–225 °C. The frequency of injection varies from 10 to 30 Hz, corresponding to rotational speeds from 1200 to 3600 rpm. The duration of injection (Δt_{inj}) is set to 5 ms and the injection pressure at 3 bar.

The time-average surface heat flux at each radial location is obtained from integration of the instantaneous heat flux, $\dot{q}''(r,0,\tau)$ over the period of injection:

$$\overline{\dot{q}''}(r,0) = f_{inj} \cdot \int_0^{T_{inj}} \dot{q}''(r,0,\tau)\mathrm{d}\tau \tag{10}$$

where T_{inj} is the cycle duration, which depends on the frequency of injection. The integral is calculated numerically using the composed trapezes rule of integration. Because of the relatively high sample rate, the integration error is negligible.

Figs. 10–12 depict the time-average wall heat fluxes measured along a radial transverse across the radial direction. In general, the results confirm the heterogeneous structure of spray impact, though showing a symmetric behavior.

Maximum overall values occur at a surface temperature which varies with the frequency of injection, suggesting the likely importance of injection conditions on the Nukiyama temperature (see Fig. 8). It is noteworthy here that the time lag between successive injections decreases when the frequency of injection increases, thus increasing the interaction of each injection with the next. While this increased interaction enhances the heat transfer at the nucleate/boiling regime, it produces negligible effects in the vicinity of the Nukiyama temperature.

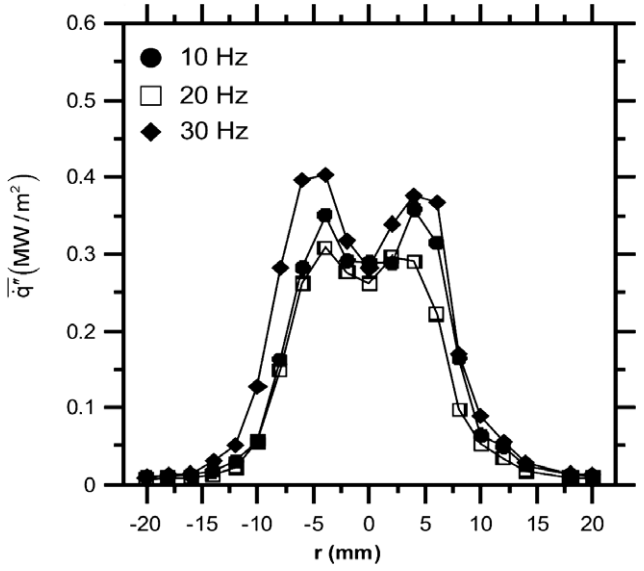

Fig. 10. Effect of injection frequency on the time-average heat flux across the radial transverse, T_w ($\xi = 0$, $\tau = 0$) = 175 °C.

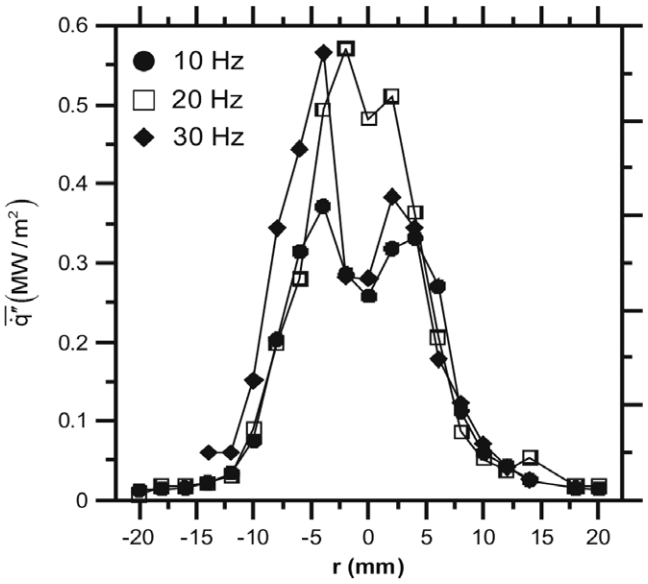

Fig. 11. Effect of injection frequency on the time-average heat flux along a radial transverse, T_w ($\xi = 0$, $\tau = 0$) = 200 °C.

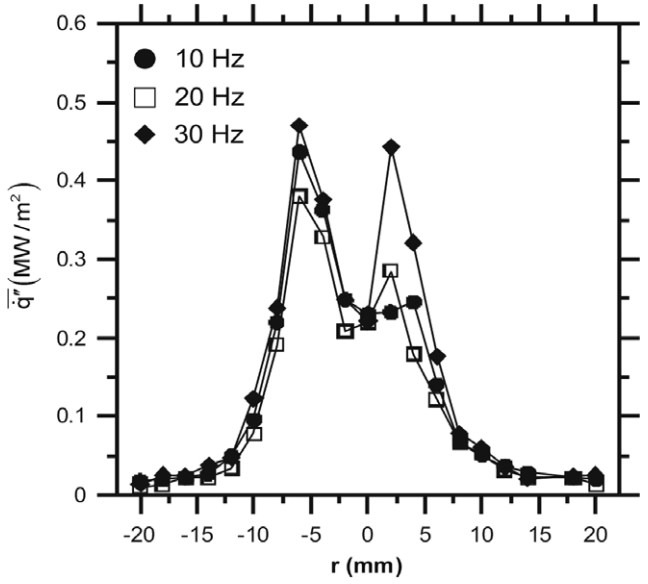

Fig. 12. Effect of injection frequency on the time-average heat flux along a radial transverse, T_w ($\xi = 0$, $\tau = 0$) = 225 °C.

A good parameter to account for the spatial non-uniform distribution of the heat transfer regimes is the efficiency of the spray cooling event, denoted here as ε. The efficiency is defined here as the ratio of the total average heat flux removed over the entire area of impact, $\langle\overline{\dot{q}''}\rangle$, to the maximum which would have been removed if all the thermal energy for complete vaporization of the spray have been received from the surface, $\langle\overline{\dot{q}''}\rangle_{max}$:

$$\langle\overline{\dot{q}''}\rangle = \frac{1}{A_{impact}} \int_0^{\pi} \int_{-R}^{R} \overline{\dot{q}''}(r,0)\mathrm{d}r\,\mathrm{d}\theta \tag{11}$$

$$\langle\overline{\dot{q}''}\rangle_{max} = \frac{\dot{m}_f \Delta t_{inj}}{T_{inj} A_{impact}} \left[C_p(T_{sat} - T_{fuel}) + L_{fg}\right] \tag{12}$$

The relative magnitude of the sensible to the latent heat was estimated to be smaller than 16.4% for all the experimental conditions.

The impact area, A_{impact}, is $\pi D_{impact}^2/4$ with $D_{impact} = 40$ mm, $\dot{m}_f$ is the mass flow rate obtained from the calibration of the injector (16 ± 1.03 mm^3/inj), T_{fuel} is the fuel temperature (32 °C), and finally, C_p and h_{fg} are the fuel specific heat and latent heat of evaporation at the reference temperature, T_r, defined as:

$$T_r(T_{fuel}) = \begin{cases} T_{sat} - \dfrac{T_{fuel} - T_{sat}}{3} & \text{if } T_{fuel} > T_{sat} \\ T_{fuel} - \dfrac{T_{sat} - T_{fuel}}{3} & \text{if } T_{fuel} < T_{sat} \end{cases} \quad (13)$$

The efficiency is then defined as:

$$\varepsilon = \frac{\langle \overline{\dot{q}''} \rangle}{\langle \overline{\dot{q}''} \rangle_{max}} \times 100\% \quad (14)$$

Fig. 13 depicts the values of $\langle \overline{\dot{q}''} \rangle$ as a function of the injection frequency. The figure shows that the total average heat flux removed by the spray increases with the injection frequency as a result of the interaction between successive injections. The values vary with the temperature of the surface and a maximum occurs at 200 °C, which is defined here as the *overall Nukiyama temperature*. Correspondingly, the temperature $T_w = 175$ °C is associated to an *overall nucleate/boiling regime* (see Fig. 3) and $T_w = 225$ °C to an *overall transition regime*.

It would be interesting at this point to infer about how the *overall Nukyiama temperature* compares to the one for local heat flux. This is shown in Fig. 14, where the radial variation of the local Nukyiama temperature is depicted, as reported in a previous paper (Panão and Moreira, 2005b). The results show that the *overall Nukyiama temperature* approaches the local Nukyiama temperature at core of the impact area where the mass rate of impinging droplets is larger ($1 < r < 2$ mm). This is due to the fact that surface dryout at the CHF starts at the outer edge of the impacted area where the volumetric flux of droplets is smaller, as described in Estes and Mudawar (1995), which increases the relative contribution of the heat removed at the inward region to the total heat flux over the entire area of impact.

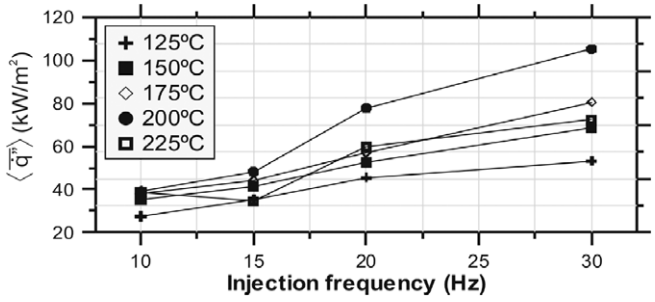

Fig. 13. Effect of the injection frequency on the total average heat flux removed by the spray.

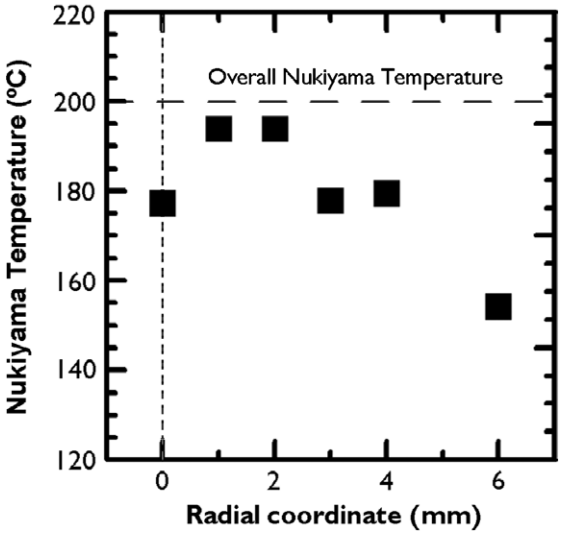

Fig. 14. Radial variations of the local Nukiyama temperature ($f = 30$ Hz, $p_{inj} = 3$ bar, $\tau_{inj} = 5$ ms).

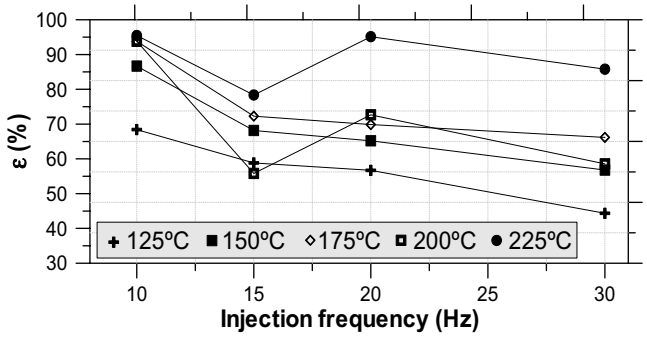

Fig. 15. Effect of the injection frequency on the thermal efficiency of the spray cooling event.

Fig. 15 depicts the variation of the thermal efficiency of the spray cooling event with the frequency of injection for several values of surface temperature at start of injection. For surface temperatures below the *overall Nukyiama temperature*, the results show that the efficiency decreases monotonically with increasing frequency, which is associated with a decreased contribution of the latent heat of vaporization. This is a clear indication that the interaction between successive injections deteriorates the rate of liquid vaporization, which is to be contrasted with observations reported by Cowart and Cheng (1999) in a real engine operating at steady-state ambient conditions similar to those considered here.

However, a different behavior is observed above the *overall Nukyiama temperature*, which is associated with the corresponding *overall heat transfer regimes* described before.

4. Conclusions

The present paper reports an experimental work aimed at the development of a systematic methodology for the

analysis of the spray cooling event which occurs at the impact of a gasoline spray onto the back surface of intake valves in port-fuel injection systems. The analysis makes use of a phase-Doppler anemometer to measure droplet characteristics at impact and fast response thermocouples to measure surface temperature in a simplified flow configuration. The practical relevance of such a methodology is to provide more accurate information on the interaction between spray characteristics and the heat transfer processes, which may be useful for the optimization of gasoline injection systems so to avoid the formation of liquid films and to improve fuel evaporation and fuel/air mixture preparation.

Simultaneous measurements of instantaneous droplets size and velocity together with surface temperature during the period of injection allowed deriving a correlation for the Nusselt number for the transient period of engine warm-up, valid for a wetting heat transfer regime:

$$Nu = 3.4 \times 10^{-5} \frac{Re^{1.51}}{Ja^{0.254}}$$

For the engine operating at steady state, an integral method is suggested to analyze the thermal behavior of intake valves upon the fuel spray impact. The methodology defines *overall boiling curves* dependant on the injection conditions (pressure, duration and frequency). Analysis showed that, although the total average heat flux removed from the surface increases with the injection frequency, the opposite occurs for the efficiency of the spray cooling event, which is attributed to the excess of liquid mass remaining at the surface between successive injections.

Acknowledgements

The authors acknowledge the financial contribution of the National Foundation of Science and Technology at the Ministry for Science and Technology to build the experimental installation through project POCTI/2001/EME/38082. The author M.R.O. Panão is also provided with financial support through PhD grant SFRH/BD/18669/2004.

References

Alkidas, A.C., 2001. Intake-valve temperature histories during SI engine warm-up. SAE Technical Paper 2001-01-1704.

Arcoumanis, C., Chang, J.-C., 1994. Flow and heat transfer characteristics of impinging transient diesel sprays. SAE Technical Paper 940678.

Arcoumanis, C., Cutter, P., 1995. Flow and heat transfer characteristics of impinging diesel sprays under cross-flow conditions. SAE Technical Paper 950448.

Arcoumanis, C., Chang, J.-C., 1993. Heat transfer between a heated plate and an impinging transient diesel spray. Experiments in Fluids 16, 105–119.

Bauer, W.D., Heywood, J.B., Bauer, P., Gronniger, S., 1997. Heat transfer and mixture vaporization in intake port of spark-ignition engine. SAE Technical Paper 972983.

Bejan, A., 1993. Heat Transfer. John Wiley & Sons, Inc., Singapore, p. 630.

Buttsworth, D.R., Jones, T.V., 1998. A fast-response high spatial resolution total temperature probe using a pulsed heating technique. Journal of Turbomachinery 120, 601–607.

Chen, X.D., Nguang, S.K., 2003. The theoretical basis of heat flux sensor. Journal of Applied Mathematics and Decision Sciences 7, 1–10.

Choi, K.J., Yao, S.C., 1987. Mechanisms of film boiling heat transfer of normally impacting spray. International Journal of Heat and Mass Transfer 30, 311–318.

Cowart, J., Cheng, W., 1999. Intake valve thermal behavior during steady-state and transient engine operation. SAE Technical Paper 1999-01-3643.

Cutter, P., 1996. Diesel spray characteristics, spray/wall interaction and heat transfer. PhD Thesis, Imperial College of Science, Technology and Medicine, University of London.

Estes, K.A., Mudawar, I., 1995. Correlation of Sauter mean diameter and critical heat flux for spray cooling of small surfaces. International Journal of Heat and Mass Transfer 38, 2985–2996.

González, J.E., Black, W.Z., 1997. Study of droplet sprays prior to impact on a heated horizontal surface. ASME Journal of Heat Transfer 119, 279–287.

Jia, W., Qiu, H.-H., 2003. Experimental investigation of droplet dynamics and heat transfer in spray cooling. Experimental Thermal and Fluid Science 27, 829–838.

Lindgren, R., Denbratt I., 2000. Modelling gasoline spray-wall interaction – a review of current models. SAE Technical Paper 2000-01-2808.

Mundo, C., Sommerfeld, M., Tropea, C., 1995. Droplet-wall collisions: experimental studies of the deformation and breakup process. International Journal of Multiphase Flow 21, 81–173.

Naber, J.D., Farrell, P.V., 1993. Hydrodynamics of droplet impingement on a heated surface. SAE Technical Papers 930919.

Panão, M.R., Moreira, A.L.N., 2002. Visualization and analysis of spray impingement under cross-flow conditions. SAE Technical Paper 2002-01-2664.

Panão, M.R.O., Moreira, A.L.N., 2004. Experimental study of the flow regimes resulting from the impact of an intermittent gasoline spray. Experiments in Fluids 37, 834–855.

Panão, M.R.O., Moreira, A.L.N., 2005a. Flow characteristics of spray impingement in PFI injection systems. Experiments in Fluids 39, 364–374.

Panão, M.R.O., Moreira, A.L.N., 2005b. Thermo-and fluid dynamics characterization of spray cooling with multiple-intermittent sprays. Experimental Thermal and Fluid Science 30, 79–96.

Reichelt, L., Meingast, U., Renz, U., 2002. Calculating transient wall heat flux from measurements of surface temperature. International Journal of Heat and Mass Transfer 45, 579–584.

Roisman, I.V., Tropea, C., 2001. Flux measurements in sprays using phase-Doppler techniques. Atomization and Sprays 11, 667–700.

Saffman, M., 1987. Automatic calibration of LDA measurement volume size. Applied Optics 26, 2592–2597.

Shayler, P.J., Colechin, M.J.F., Scarisbrick, A., 1996. Fuel film evaporation and heat transfer in the intake port of an S.I. engine. SAE Technical paper 961120.

Sowa, W.A., 1992. Interpreting mean drop diameters using distribution moments. Atomization and Sprays 2, 1–15.

Tate, R.W., 1982. Some problems associated with the accurate representation of droplet size distributions. In: Proceedings of the Second International Conference on Liquid Atomic and Spray Systems, Madison.

Yao, S.C., Choi, K.J., 1987. Heat transfer experiments of mono-dispersed vertically impacting sprays. International Journal of Multiphase Flow 13, 639–648.

Yoshida, K., Abe, Y., Oka, T., Mori, Y.H., Nagashima, A., 2001. Spray cooling under reduced gravity conditions. ASME Journal of Heat Transfer 123, 309–318.